UNVEILING THE STRUCTURAL FEATURES OF THE OUTER MILKY WAY DISC

Ž. Chrobáková, zofia.chrobakova@fmph.uniba.sk, Faculty of Mathematics, Physics, and Informatics, Comenius University, Mlynská dolina, 842 48 Bratislava, Slovakia

INTRODUCTION

Understanding the Milky Way's structure is vital for astronomy, with star counts as a crucial technique. Wide-area surveys like those by [1] and [2] have improved our insights into the Galactic thin and thick discs and halo. However, these surveys highlight the need to consider asymmetric features seen in 3D star distributions, e.g., [3] and [4].

One of such features is the Galactic warp, which is a distortion of the Galactic disc from the flat shape to a shape resembling the letter "S". The warp was initially detected in the Galactic gaseous disc through 21 cm HI observations [5, 6]. Later, it was identified in the stellar disc as well [7, 8, 9], prompting studies into its kinematics [10, 11, 12].

The warp's precise shape remains roughly constrained, with no consensus on its formation mechanism. Among the proposed theories is intergalactic matter accretion onto the disc [13], satellite interactions [14], influence of the intergalactic magnetic field [15] or a misaligned rotating halo [16].

Recent investigations have delved into the kinematics and evolution of the Galactic warp to unravel its origins [17, 18, 19]. Especially the result of [18] is of great significance, since it is the first measurement of the precession of the Galactic warp. Using data from the second Gaia data release DR2 [20, 21] combined with Two Micron All-Sky Survey [22, 2MASS] photometry, they determined the warp's precession to be $\beta = 10.86 \pm 0.03(stat.) \pm 3.20(syst.)$ km s^{-1} kpc^{-1}. Notably, this finding significantly exceeds predictions derived from various warp formation mechanisms, which predict a relatively low precession rate between 0.1 and 1.5 km s^{-1} kpc^{-1}. Therefore, the results obtained by [18] challenge the conclusions drawn from dynamical models of warp formation, implying that the warp might not be a slowly evolving structure but rather a transient response of the disc to external influences. Given that most spiral galaxies exhibit warps [23, 24], it seems improbable that these warps are solely attributed to transient phenomena unless a widespread triggering substructure exists in these galaxies.

DATA SELECTION

We used Gaia mission's second data release (DR2), spanning 22 months of observations, focusing on stars with well-determined five-parameter astrometric solutions, totalling over 1.3 billion sources with G magnitudes measured in Gaia's white-light G-band (330-1050 nm). We specifically selected stars with apparent magnitudes up to G=19, ensuring up to 90% catalogue completeness [25]. Our choice was limited to stars with parallaxes in the [0, 2] mas range. Detailed astrometric data processing and validation methods can be found in [26].

For radial velocity data, we utilised the dataset provided by [27], who derived the Milky Way kinematic maps from Gaia DR2. This dataset included stars with both radial heliocentric velocities and parallaxes, having errors below 100%, totaling 7,103,123 sources. These stars were observed using the Radial Velocity Spectrometer [28, RVS]. From the initial sample, we further filtered stars with Galactic latitudes $|b| < 10°$, Galactocentric distances $R > 12$ kpc, and heliocentric distances $r < 8$ kpc. This filtering resulted in a dataset covering Galactocentric radii from $12 < R < 16$ kpc, reaching a maximum vertical distance of approximately $z \sim 1.4$ kpc and an angular range of $|\phi| < 40°$.

DENSITY MAPS

According to the equation of stellar statistics [29], the stellar density can be calculated as

$$\rho(1/\pi) = \frac{N(\pi)\pi^4}{\Delta\pi\omega \int_{M_{G,low\ lim}}^{M_{G,low\ lim}+1} \mathrm{d}M_G \Phi(M_G)} \ , \qquad (1)$$

where

$$\begin{aligned} M_{G,low\ lim} &= m_{G,low\ lim} - 5log_{10}(1/\pi) - 10 \\ &- A_G(1/\pi) \ , \end{aligned}$$

and $N(\pi)$ are the star counts as a function of the parallax, $\Delta\pi$ is the interval of the parallax (0.01 mas in our case), ω is the covered angular surface (10 degrees^2 in our case), $\Phi(M_G)$ is the luminosity function in the G filter, $m_{G,low\ lim}$ is the limiting maximum apparent magnitude, and $A_G(r)$ is the extinction, as a function of the distance. The details of the luminosity function and extinction that we applied are described in [30]. However, the star counts that we need for the calculation are not the star counts observed from the Gaia, but rather a following convolution

$$\overline{N}(\pi) = \int_0^\infty \mathrm{d}\pi' N(\pi') G_{\pi'}(\pi - \pi') \ , \qquad (2)$$

where

$$G_\pi(x) = \frac{1}{\sqrt{2\pi}\sigma_\pi} e^{-\frac{x^2}{2\sigma_\pi^2}} \ . \qquad (3)$$

To perform the deconvolution, we apply the Lucy's deconvolution method [31], which is a Bayesian iterative method, described in great detail in [27] and [30]. Then we use Eq. 1 to derive the density maps of the Galaxy in Galactocentric cylindrical coordinates. In

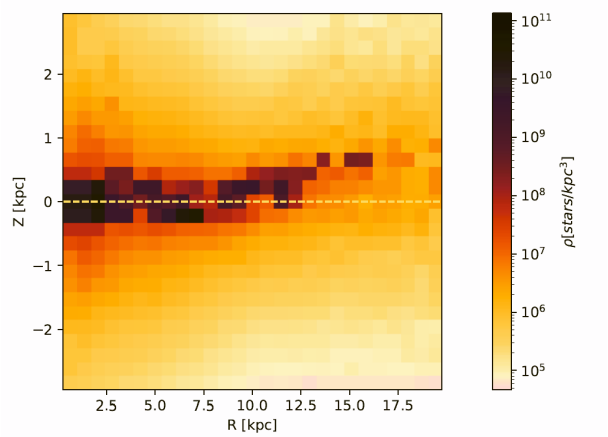

(b) $30° < \phi < 60°$

Fig. 1: Density map in Galactocentric coordinates for $30° < \phi < 60°$.

Fig. 1 we show an example of a density map for the region $30° < \phi < 60°$.

WARP ANALYSIS

We use the obtained density maps to analyse the Galactic warp. We exclude the azimuths $150° < \phi < 240°$ and radii $R < 6$ kpc from our analysis, as these data are of low quality due to significant extinction. We calculated the average elevation above the plane as

$$z_w = \frac{\int_{z_{min}}^{z_{max}} \rho z \mathrm{d}z}{\int_{z_{min}}^{z_{max}} \rho \mathrm{d}z} \tag{4}$$

and fitted it with a warp model from [32]

$$z_w = z_0 + z_1 \cdot \sin(\phi - \phi_1) + z_2 \cdot \sin(2\phi - \phi_2) \ , \tag{5}$$

where z_w is the average elevation above the plane, z_i for $i \in (0, 1, 2)$ are the amplitudes of the warp and ϕ_i for $i \in (1, 2)$ are the phases. The dependence of the amplitudes of the warp on the Galactocentric distances is

$$\begin{aligned} z_i &= k_0 + k_1 \cdot (R - R_k) + k_2 \cdot (R - R_k)^2 \\ i &= 0, 1, 2 \ , \end{aligned} \tag{6}$$

where k_i and R_k are free parameters of the fit. An example of the warp can be see in Fig. 2, where we plot the fit at a distance $R = 17.25$ kpc.

The result of the fit compared to other works can be seen in Fig. 3, where we can observe that the warp that we obtain is much lower than that of the other authors. The other works that reach a distance of 20 kpc are works of [4, 9] that use Cepheids, which are a particular stellar population of very young stars, with ages $\sim$ Myr, while our dataset represents the average stellar population of the thin disc with ages $\sim 5{-}6$ Gyr. Since our older population has a much smaller warp, it is clear that the amplitude of the warp is strongly dependent on the age of the stellar population.

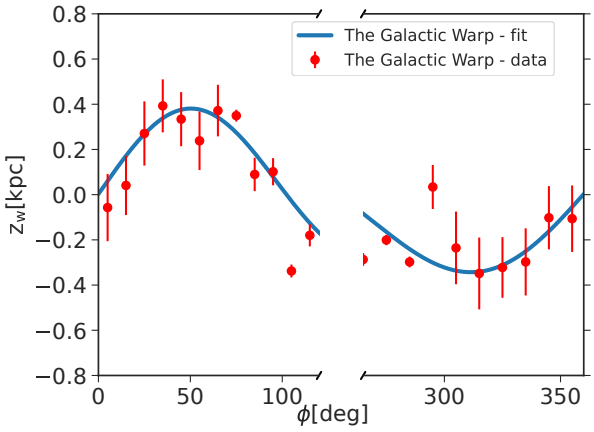

Fig. 2: Average elevation above the plane (red), fitted by the warp model (blue) at a Galactocentric distance $R = 17.25$ kpc.

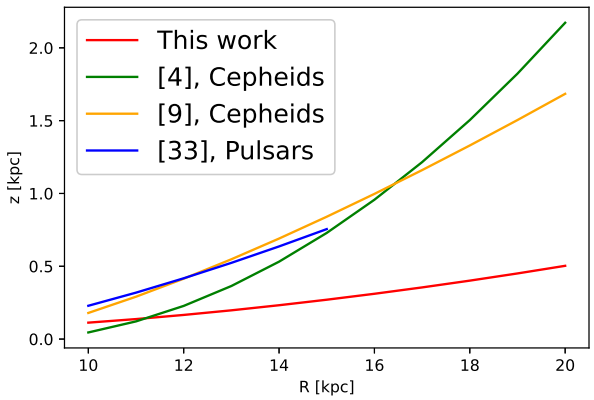

Fig. 3: The maximum amplitude of the warp, compared with values from the literature.

WARP PRECESSION

The warp model that we obtained can be used to measure the precession of the Galactic warp. As in this section we are exploring smaller distances up to $R = 16$ kpc, we use a more simple model as follows:

$$z_w = [C_w R(pc)^{\epsilon_w} \sin(\phi - \phi_w) + 17] \ pc \ . \tag{7}$$

This model conceptualises the warp as a collection of tilted rings, with the tilt determined by the Galactocentric distance raised to the power of ϵ_w. The parameters of the model - the amplitude C_w, ϵ_w, and the angle defining the line of nodes ϕ_w were fitted in a previous study by [30]. The term 17 pc compensates for the Sun's elevation above the Galactic plane [34].

We account for the time evolution of the warp amplitude (C_w) and warp precession (ϕ_w) with the following equations:

$$C_w(t) = C_{w,max} \sin(\omega t + \alpha) \ , \tag{8}$$

$$\phi_w(t) = \phi_{w0} + \beta t \ . \tag{9}$$

We adopt the approach of [18], which involves taking the zeroth moment of the collisionless Boltzmann

equation to derive the expression for the vertical velocity. The resulting formula for the vertical velocity is

$$\begin{aligned} v_z(R,\phi) &= C_{w,0} K R^{\epsilon_w} \sin(\phi - \phi_{w,0}) \\ &- C_{w,0} R^{\epsilon_w} \beta \cos(\phi - \phi_{w,0}) \\ &+ C_{w,0} R^{\epsilon_w - 1} \cos(\phi - \phi_{w,0}) v_\phi \ , \end{aligned} \tag{10}$$

where $C_{w,0}$ and $\phi_{w,0}$ are values at the present time t obtained from equations (8) and (9), and

$$K = \omega \cdot \mathrm{cotan}(\alpha) \ . \tag{11}$$

Initially, we only analysed data in the anticentre ($|\phi| < 10°$). In this case, the dependence of amplitude on time is negligible, as can be seen from Eq. (10), when the value of the angle of the line of nodes is set. Consequently, we only have one free parameter, β, representing the precession of the warp's azimuth (Eq. (9)).

In Figure 4(a), we present the best-fit results along with the non-precessing warp for the model of [18]. It is evident that the non-precessing model, due to its high amplitude, produces velocities considerably higher than the observed data. Hence, a substantial precession is necessary to fit the data. In contrast, as shown in Figure 4(b), a non-precessing warp already yields velocities roughly in line with the data, with precession contributing only minor corrections. The precession value obtained with model of [18] is $\beta = 13 \pm 1$ km s^{-1} kpc^{-1}, which is similar, albeit slightly higher, than the result of [18] ($\beta = 10.86 \pm 0.03(stat.) \pm 3.20(syst.)$ km s^{-1} kpc^{-1}), likely due to dataset differences. The precession value derived from the old stellar population of Gaia DR2 is $\beta = -1 \pm 9$ km s^{-1} kpc^{-1}, consistent with both the non-precessing warp model and the result of [18], given the large error bars.

Next, we conducted a comprehensive fit with all azimuthal angles, utilising the complete model given by Eq. (10), which accounts for precession and time-dependent warp amplitude variation. Indeed, according to the literature, the variation in warp amplitude might be more important than the precession term [11, 35]. In this scenario, we found that the best-fit values are $K = 16^{+12}_{-8}$ km s^{-1} kpc^{-1} and $\beta = 4^{+6}_{-4}$ km s^{-1} kpc^{-1}, so in this case we cannot constrain the parameters either.

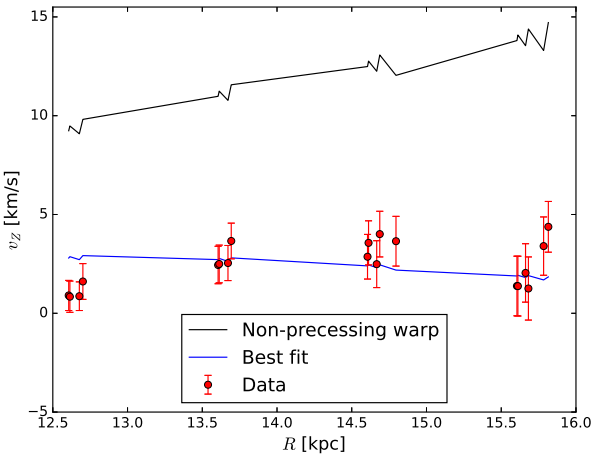

(a)

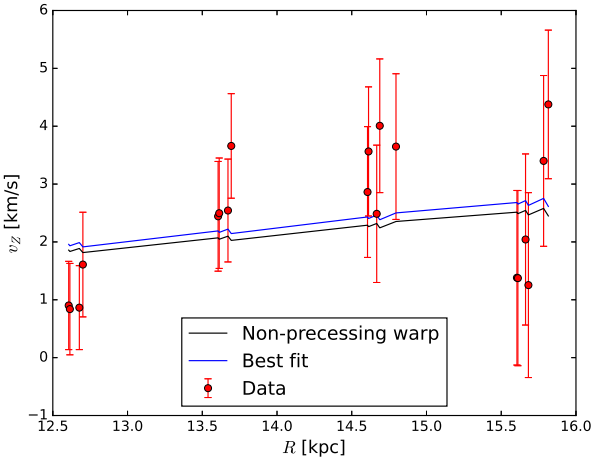

(b)

Fig. 4: Vertical velocity (red), fitted by a precessing warp model(blue). A warp without precession is also depicted (black). (a) Fit for the model of [18]. (b) Fit derived in this work.

CONCLUSIONS

We utilized Gaia DR2 data to generate density maps and conducted an in-depth analysis to investigate the Galactic warp. Our maps extend to an unprecedented Galactocentric radius of 20 kpc, where we observed no density cut-off; instead, the density exhibits an exponential decrease. To study the warp's characteristics without assuming its presence, we calculated the average deviation of the Galactic plane and applied a model combining two sinusoidal components to discern any asymmetry in the warp.

In terms of Galactocentric radius, we detected the warp's emergence starting at approximately 12 kpc, and it extends, at least, up to 20 kpc. Comparing our warp amplitude with other studies, we found that our measurements yield a significantly lower amplitude than the previous studies that used very young stars such as Cepheids. This supports the hypothesis of warp formation through accretion onto the Galactic disc [30].

Additionally, we explored a much-debated topic of the past years: the precession of the Galactic warp. Our calculations were built on the model of [18], but using the warp model derived in this work. The models employed by [18] were derived for a much younger stellar population (approximately a few million years) and as we showed, warp is strongly dependent on the age of the studied population.

When we considered this dependence, we found

that our best-fit results were compatible with the absence of precession. However, we did not uncover evidence neither supporting nor excluding a specific model for warp formation. Therefore, we need future studies to shed light on the kinematics of the warp and, subsequently, its formation mechanism.

ACKNOWLEDGMENT: The author was supported by VEGA—the Slovak Grant Agency for Science, grant No. 1/0761/21, and by the Erasmus+ programme of the European Union under grant No. 2020-1-CZ01-KA203-078200. This work made use of the IAC Supercomputing facility HTCondor (http://research.cs.wisc.edu/htcondor/), partly financed by the Ministry of Economy and Competitiveness with FEDER funds, code IACA13-3E-2493. This work has made use of data from the European Space Agency (ESA) mission *Gaia* (`https://www.cosmos.esa.int/gaia`), processed by the *Gaia* Data Processing and Analysis Consortium (DPAC, `https://www.cosmos.esa.int/web/gaia/dpac/consortium`).

REFERENCES

1. J. N. Bahcall, Annual Review of Astronomy and Astrophysics, **24**, 577 (1986).
2. S. R. Majewski, Annual Review of Astronomy and Astrophysics, **31**, 575 (1993).
3. C. Liu, Y. Xu, J.-C. Wan, et al., Research in Astronomy and Astrophysics, **17**, 096 (2017).
4. D. M. Skowron, J. Skowron, P. Mróz, et al., Science, **365**, 478 (2019).
5. F. J. Kerr, Astronomical Journal, **62**, 93 (1957).
6. J. H. Oort, F. J. Kerr, and G. Westerhout, Monthly Notices of the Royal Astronomical Society, **118**, 379 (1958).
7. B. W. Carney and P. Seitzer, Astronomical Journal, **105**, 2127 (1993).
8. M. López-Corredoira, A. Cabrera-Lavers, F. Garzón, and P. L. Hammersley, Astronomy & Astrophysics, **394**, 883 (2002).
9. X. Chen, S. Wang, L. Deng, et al., Nature Astronomy, **3**, 320 (2019).
10. W. Dehnen, Astronomical Journal, **115**, 2384 (1998).
11. M. López-Corredoira, H. Abedi, F. Garzón, and F. Figueras, Astronomy & Astrophysics, **572**, A101 (2014).
12. R. Schönrich and W. Dehnen, Monthly Notices of the Royal Astronomical Society, **478**, 3809 (2018).
13. M. López-Corredoira, J. Betancort-Rijo, and J. E. Beckman, Astronomy & Astrophysics, **386**, 169 (2002).
14. J. H. Kim, S. Peirani, S. Kim, et al., The Astrophysical Journal, **789**, 90 (2014).
15. E. Battaner, E. Florido, and M. L. Sanchez-Saavedra, Astronomy & Astrophysics, **236**, 1 (1990).
16. V. P. Debattista and J. A. Sellwood, The Astrophysical Journal, **513**, L107 (1999).
17. E. Poggio, R. Drimmel, M. G. Lattanzi, et al., Monthly Notices of the Royal Astronomical Society, **481**, L21 (2018).
18. E. Poggio, R. Drimmel, R. Andrae, et al., Nature Astronomy, **4**, 590 (2020).
19. H.-F. Wang, M. López-Corredoira, Y. Huang, et al., The Astrophysical Journal, **897**, 119 (2020).
20. Gaia Collaboration, T. Prusti, J. H. J. de Bruijne, A. G. A. Brown, et al., Astronomy & Astrophysics, **595**, A1 (2016).
21. Gaia Collaboration, A. G. A. Brown, A. Vallenari, T. Prusti, et al., Astronomy & Astrophysics, **616**, A1 (2018).
22. M. F. Skrutskie, R. M. Cutri, R. Stiening, et al., Astronomical Journal, **131**, 1163 (2006).
23. V. Reshetnikov and F. Combes, Astronomy & Astrophysics, **337**, 9 (1998).
24. M. L. Sánchez-Saavedra, E. Battaner, A. Guijarro, M. López-Corredoira, and N. Castro-Rodríguez, Astronomy & Astrophysics, **399**, 457 (2003).
25. F. Arenou, X. Luri, C. Babusiaux, et al., Astronomy & Astrophysics, **616**, A17 (2018).
26. L. Lindegren, J. Hernández, A. Bombrun, et al., Astronomy & Astrophysics, **616**, A2 (2018).
27. M. López-Corredoira and F. Sylos Labini, Astronomy & Astrophysics, **621**, A48 (2019).
28. M. Cropper, D. Katz, P. Sartoretti, et al., Astronomy & Astrophysics, **616**, A5 (2018).
29. S. Chandresekhar, G. Münch, The Astrophysical Journal, **113**, 150 (1951).
30. Ž. Chrobáková, R. Nagy, and M. López-Corredoira, Astronomy & Astrophysics, **637**, A96 (2020).
31. L. B. Lucy, Astronomical Journal, **79**, 745 (1974).
32. E. S. Levine, L. Blitz, and C. Heiles, The Astrophysical Journal, **643**, 881 (2006).
33. I. Yusifov, The Magnetized Interstellar Medium, 165 (2004).
34. T. Karim and E. E. Mamajek, Monthly Notices of the Royal Astronomical Society, **465**, 472 (2017).
35. M. López-Corredoira, F. Garzón, H.-F. Wang, et al., Astronomy & Astrophysics, **634**, A66 (2020).